Downloaded from rsta.royalsocietypublishing.org

PHILOSOPHICAL TRANSACTIONS OF THE ROYAL SOCIETY A MATHEMATICAL, PHYSICAL & ENGINEERING SCIENCES

^{13}C n.m.r. in Organic Solids: Limits to Spectral Resolution and to Determination of Molecular Motion [and Discussion]

A. N. Garroway, D. L. Vander Hart, W. L. Earl and W. S. Veeman

Phil. Trans. R. Soc. Lond. A 1981 **299**, 609-628
doi: 10.1098/rsta.1981.0038

Email alerting service

Receive free email alerts when new articles cite this article - sign up in the box at the top right-hand corner of the article or click **here**

To subscribe to *Phil. Trans. R. Soc. Lond. A* go to: **http://rsta.royalsocietypublishing.org/subscriptions**

This journal is © 1981 The Royal Society

Downloaded from rsta.royalsocietypublishing.org

Phil. Trans. R. Lond. A **299**, 609–628 (1981)
Printed in Great Britain

^{13}C n.m.r. in organic solids: limits to spectral resolution and to determination of molecular motion

By A. N. Garroway,† D. L. VanderHart‡ and W. L. Earl‡
† *Chemistry Division, Naval Research Laboratory, Washington, D.C.* 20375, *U.S.A.*
‡ *National Bureau of Standards, Washington, D.C.* 20234, *U.S.A.*

The history of high-resolution n.m.r. in solids has been, *inter alia*, a quest for narrow spectral lines. Yet, with few exceptions, solid state resonances have not been sharpened to the degree of liquid resonances. To aid in the appraisal of the status of n.m.r. in solids, we identify and summarize, for the particular case of ^{13}C n.m.r. in organic solids, those effects that can degrade resolution. Some of these mechanisms are under the experimenter's control; for example, certain are exacerbated at high magnetic field. Others, however, represent fundamental limitations imposed by the specimen and are valid reflections of the complexity of a solid as contrasted to a liquid.

In solids, magnetic dipolar spin–spin couplings can not only degrade resolution but also complicate, hopelessly in some cases, the determination of spin–lattice relaxation rates from which one seeks information about molecular motions. The consequences of this competition between spin–spin and spin–lattice effects are examined, as well as criteria and strategies to isolate the motional contributions to relaxation rates.

1. Introduction

The n.m.r. spectroscopy of organic solids is based on principles well established 20 years ago and earlier. Cross-polarization and spin dynamics in heteronuclear systems generally derive from the work of Bloembergen & Sorokin (1958), Bloembergen *et al.* (1959) and from the classic paper of Hartmann & Hahn (1962), while heteronuclear dipolar decoupling was examined theoretically and experimentally by Bloch and coworkers (Bloch 1958; Sarles & Cotts 1958). Magic angle sample spinning was introduced independently by Lowe (1959) and Andrew (1959); fuller accounts of sample spinning and its applications appear in the paper by Professor Andrew and in other papers in this symposium. Yet not until recently were these techniques merged into a practicable, readily implemented and powerful combination that achieves high-resolution ^{13}C spectra in solids. Pines *et al.* (1972, 1973*a*, *b*) demonstrated convincingly the utility of direct detection cross-polarization for simple organic crystals. Schaefer & Stejskal (1976) added to this method magic angle sample spinning to extend the range of applicability to intractable polymers.

It remains to the student of science history to account for the rather long delay between the first experimental demonstrations in inorganic crystals 20 years ago and the widespread acceptance of solid state ^{13}C methods; commercial spectrometers, equipped for cross-polarization and magic angle sample spinning, have appeared only within the last few years. Clearly today's vigorous development in this field is based as much on the remarkable progress in *liquid* state Fourier transform spectroscopy, a progress that has educated recently trained organic chemists to rely upon high-quality, easily obtained ^{13}C spectra.

The coming decade will, most likely, see further deployment of these solid state spectrometers. Many applications of these techniques are described elsewhere within the symposium. In this paper we address the questions of limitations on spectral resolution and on determination of

The Royal Society is collaborating with JSTOR to digitize, preserve, and extend access to *Philosophical Transactions of the Royal Society of London. Series A, Mathematical and Physical Sciences.* www.jstor.org

Downloaded from rsta.royalsocietypublishing.org

molecular motions in solid state experiments: what present limitations are and whether they are likely to moderate in the future. (A corollary asks, in the light of the availability of solenoids of ever-increasing field strength, how these limitations depend on static field.)

No review of limitations can be comprehensive. We identify here the mechanisms that we have found to dominate for the particular case of crystalline and amorphous organic solids. Excluded is any consideration of elastomeric systems examined above T_g; nor do we examine problems particular to the complexities of coal (Bartuska *et al.* 1977; T. Taki, personal communication, 1979) and oil shale (Resing *et al.* 1978).

Any success in identification of the limitations can be attributed to the historical development just sketched; though there is high excitement over novel applications, the theoretical understanding is comparatively mature. To appreciate most of the limitations, one may appeal to rather well accepted notions. There are still puzzling features, even in such a pedestrian topic as limitations. It should also be recognized that we address these limitations in the narrow context of particular n.m.r. techniques; these restrictions may vanish trivially by another approach.

We now examine two categories of n.m.r. experiments: rotating frame relaxation and the resolution of spectral lines. The dynamics of rotating frame relaxation are sensitive to frequencies at the nutational rate of the effective r.f. field; this rate is typically within the range 10–100 kHz. On the other hand, features in a spectrum are frequently determined by much lower frequencies, characteristic of the line width. However, in the ^{13}C experiments, two coherent averaging strategies (magic angle sample spinning and dipolar decoupling) are simultaneously applied and so spectral resolution can be degraded by frequencies at the spinning and decoupling frequencies. Hence these two problems present many common features. First we consider rotating frame relaxation in § 2 and then examine resolution in § 3.

In the experiments reported here, two separate home-built solid state ^{13}C spectrometers were used. Both operate at 1.4 T. One uses a modified Lowe spinner geometry (Lowe 1959), has variable temperature facility and employs r.f. fields up to 66 kHz on both proton and carbon channels. The other uses a Beams–Andrew spinner (Andrew 1959) and achieves r.f. field strengths up to 83 kHz.

2. Rotating frame relaxation

(*a*) *Spin–lattice and spin–spin relaxation*

In strongly coupled organic solids, proton spin diffusion tends to homogenize any intrinsically disparate proton spin–lattice relaxation rates. In principle, and often in practice, carbon spin–lattice relaxation times are site-specific (Schaefer *et al.* 1977; Stejskal *et al.* 1979; Garroway *et al.* 1979*a*, *b*; VanderHart & Garroway 1979; Schaefer *et al.* 1980; Earl & VanderHart 1979). Carbon–carbon spin diffusion times are rather long for ^{13}C nuclei at natural abundance in typical organic solids, as the carbon–carbon dipolar coupling is quite small, though not always negligible, in comparison with carbon–proton or proton–proton couplings. The complicating factor is that unless the carbon r.f. field strength, which determines the rotating frame Zeeman energy levels, is sufficiently large, an alternative relaxation pathway will compete successfully with the rotating frame spin–lattice relaxation (Schaefer *et al.* 1977; Stejskal *et al.* 1979; Garroway *et al.* 1979*a*, *b*; VanderHart & Garroway 1979; Schaefer *et al.* 1980). This alternative proceeds by spin–spin fluctuations that transfer energy between the carbon rotating frame Zeeman levels and the dipolar reservoir, made up in these experiments by the proton–proton couplings. Such a process is well documented in simple single crystals and their powders (Hartmann & Hahn 1962;

Downloaded from rsta.royalsocietypublishing.org

McArthur *et al.* 1969; Pines & Shattuck 1974; Stokes & Ailion 1977). Its diagnostic value has not been established in polymer systems and our view here is that this spin–spin pathway is an unnecessary complication that should be reduced to a minimum: interpretation of the pure mechanism of relaxation by molecular motion in solids, unencumbered by spin–spin effects, is formidable on its own. We examine below, in qualitative fashion, the origin and some consequences of this mechanism; fuller analyses are found in the references cited.

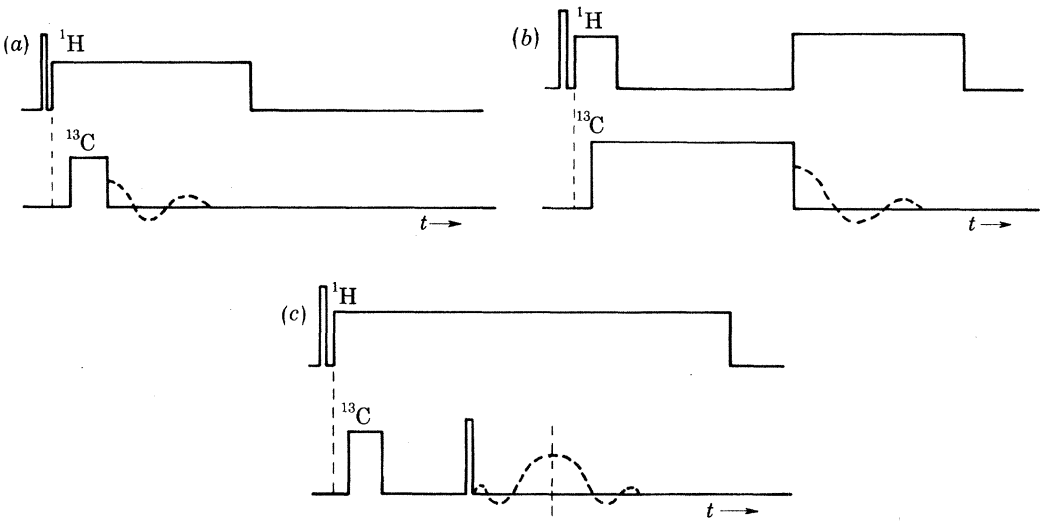

FIGURE 1. The r.f. pulse sequence for determination of (*a*) cross-polarization time constant under spin-lock conditions with $\omega_{1C} = \omega_{1H}$ (Hartmann & Hahn 1962); (*b*) rotating frame ^{13}C relaxation time $T_{1\rho}^{C*}$ and (*c*) ^{13}C T_2 relaxation time under proton decoupling. The spin echo may be synchronized to the sample rotation. Here each sequence starts with a spin-lock cross-polarization.

For reference, figure 1 shows three representative experiments: cross-polarization, carbon spin-locking and a carbon spin-echo sequence with simultaneous dipolar decoupling (Garroway *et al.* 1979*a*). We are concerned at the outset with the spin-locking sequence that initially transfers polarization from the proton to the carbon rotating frame Zeeman level under matched spin-lock conditions (Hartmann & Hahn 1962). The resonant proton field is then removed for a variable time and the decay of carbon magnetization is followed for each line in the Fourier transformed spectrum.

In a coordinate system rotating at the carbon static field Larmor frequency $\omega_{0C} = -\gamma_C B_0$, the carbon spin-lock magnetization appears stationary along the r.f. axis. Any magnetic fields perpendicular to this axis will cause a precession and, for randomly fluctuating fields, lead to a decay of spin magnetization. All spin variables are subject to the static field B_0, imposing frequencies of ω_{0C}, $2\omega_{0C}$, ω_{0H}, $2\omega_{0H}$ and $|\omega_{0H} \pm \omega_{0C}|$ on components of the carbon–carbon, proton–proton and carbon–proton dipolar couplings perpendicular to B_0. These non-secular terms oscillate too quickly to contribute substantially to rotating frame relaxation. As for the static components along B_0, the proton–proton coupling does not *directly* influence the carbons. The strong carbon spin-locking field B_{1C} impresses a second time dependence so that proton–carbon dipolar fields initially along B_0 will precess about the r.f. field direction at the rate $\omega_{1C} = -\gamma_C B_{1C}$. When this precession is sufficiently rapid, the carbon magnetization is effectively decoupled from the carbon–proton interaction. Random fluctuations or indeed any coherent fluctuations

Downloaded from rsta.royalsocietypublishing.org

of magnetic fields perpendicular to the carbon r.f. axis with frequencies in the vicinity of ω_{1C} will lead to effectively time-independent fields that then relax the carbon magnetization (Bloembergen *et al.* 1948). Molecular motions that modulate the carbon–proton interaction $I_z S_z$ will lead to dissipation of the spin-lock magnetization into lattice or local modes. (I_z and S_z refer respectively to proton and carbon spin operators along the B_0 direction and here $I_z S_z$ is a shorthand representation for the heteronuclear dipolar Hamiltonian, summed over all appropriate spins and containing spatial as well as spin variables.)

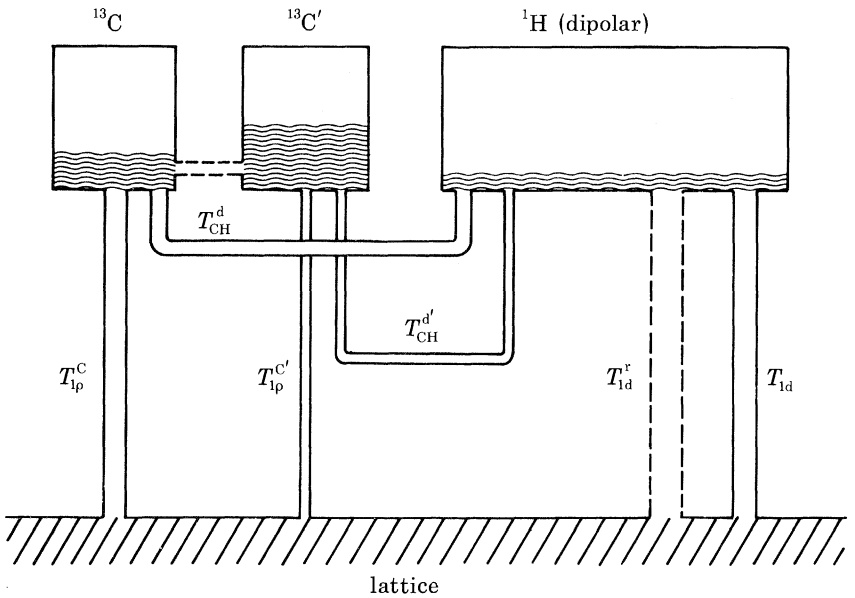

FIGURE 2. During the ^{13}C $T_{1\rho}$ experiment the various carbon rotating frame spin-lock reservoirs are in thermal contact with the lattice via $T_{1\rho}^{c}$, with the laboratory frame dipolar system via T_{CH}^{d} and very weakly with one another. Here only two carbon reservoirs are shown, corresponding to two spectrally resolved lines with different (primed and unprimed) relaxation rates. The carbon r.f. field stirs out the carbon–proton dipolar coupling and so the dipolar reservoir comprises only proton–proton ordering. The dipolar system relaxes to the lattice with T_{1d}. The parallel relaxation pathway T_{1d}^{r} represents a spin–spin dephasing of the dipolar system driven by mechanical specimen rotation. After initial transients have decayed, the behaviour of the rotating frame magnetization is determined by the interplay of the relative relaxation rates and relative populations. In the text the *observed* rotating frame relaxation time is $T_{1\rho}^{C*}$.

The dipolar Hamiltonian may also fluctuate in the absence of molecular motion. In tightly coupled systems, the protons undergo spin exchange; for many strongly coupled spins, these fluctuations are in some, but not all, respects random (Rhim *et al.* 1970). The proton–proton spin fluctuations are mirrored in the spin fluctuation spectrum of $I_z S_z$ and so spin fluctuations at ω_{1C} lead to a coupling of the rotating frame carbon system to the proton–proton dipolar reservoir. Spin–spin effects present certain distinguishing features, which we shall elaborate: (i) the spin fluctuation spectrum has a distinctly different shape from the motional fluctuation spectrum, and (ii) in contrast to the lattice, the dipolar reservoir is not infinitely large and its temperature is influenced strongly by the cross-polarization procedure as well as by mechanical sample rotation.

Most features of the competition between spin–lattice and spin–spin relaxation are present in a simplified reservoir picture (figure 2) (Garroway *et al.* 1979*a*; VanderHart & Garroway 1979). The carbon rotating frame reservoir is connected by motional processes to the lattice with a time constant $T_{1\rho}^{C}$. It is also linked to the proton–proton dipolar system by the carbon–proton spin–

Downloaded from rsta.royalsocietypublishing.org

spin relaxation time T_{CH}^{d}, where the superscript d denotes dipolar. (This time constant is elsewhere denoted as $T_{CH}^{a.d.r.f.}$, as it is the cross-polarization time to a state of carbon spin-lock order from a state of dipolar order prepared by proton adiabatic demagnetization in the rotating frame (Schaefer *et al.* 1977, 1980; Stejskal *et al.* 1979).) The dipolar reservoir is then connected to the lattice by the spin–lattice relaxation time T_{1d}, as well as a second relaxation time T_{1d}^{r}, produced by mechanical sample rotation.

For concreteness, representative relaxation rates are given in the following. For resonant carbon irradiation (VanderHart & Garroway 1979),

$$(T_{1\rho}^{C})^{-1} = \tfrac{1}{2}\langle M_{CH}^{(2)}\rangle_{m} J_{m}(\omega_{1C}), \tag{1}$$

where $\langle M_{CH}^{(2)}\rangle_{m}$ is the truncated carbon–proton second moment modulated by the motion and the motional spectral density is presumed Lorentzian with a single correlation time τ_c (Bloembergen *et al.* 1948):

$$J_{m}(\omega) = 2\tau_c/(1+\omega^2\tau_c^2). \tag{2}$$

When molecular motion can be ignored, the spin–spin relaxation time constant between the dipolar and carbon spin-lock systems is (Demco *et al.* 1975; Mehring 1976 and references therein)

$$(T_{CH}^{d})_0^{-1} = \tfrac{1}{2} M_{CH}^{(2)} J_{d}(\omega_{1C}), \tag{3}$$

where here $M_{CH}^{(2)}$ is the rigid lattice truncated carbon–proton second moment. The dipolar fluctuation spectrum is taken to be exponential

$$J_{d}(\omega) = \pi\tau_{d}\exp(-|\omega|\tau_{d}), \tag{4}$$

with $\tau_{d} \equiv (2/N_2)^{\frac{1}{2}}$. The second moment-like term N_2 involves both proton–proton and carbon–proton couplings and is given explicitly in Mehring (1976) and VanderHart & Garroway (1979). For highly anisotropic motion or for motion not fast enough to cause substantial narrowing, only slight modifications to (3) and (4) are required.

In a static sample the dipolar reservoir relaxes to the lattice with a time constant T_{1d} determined by molecular motion; for the case of slow motion and strong collisions, T_{1d} is directly proportional to the molecular jump or reorientation time (Ailion & Slichter 1965). Under rigid body mechanical rotation about any axis that is not precisely parallel to B_0, not all the spins are able to follow adiabatically the apparent motion of the local dipolar fields. Owing to this viscous force the dipolar reservoir can be rapidly depleted, even before one full mechanical revolution (Jeener 1977*a*, *b*; Pourquie & Wind 1976). For a polycrystalline specimen rotating at Ω_{rot} perpendicular to B_0, then T_{1d}^{r}, averaged over all orientations in the powder, is given by (Garroway 1979)

$$(T_{1d}^{r})^{-1} = \tfrac{1}{2}\pi\, 3\Omega_{rot}^{2}\tau_{d}', \tag{5}$$

where $\tau_{d}' \equiv (3/M_{HH}^{(2)})^{\frac{1}{2}}$ is a dipolar fluctuation time, in this case determined by the proton–proton second moment. No explicit calculation is available at the magic angle, but for spinning that is still slow compared with the proton–proton dipolar strength, we have found that the decay time is not too much different from that for perpendicular spinning. For typical strongly protonated organic solids spun at 2 kHz, dipolar order decays in a timescale of 100 μs; the decay time is shorter for more weakly coupled systems. At higher speeds (3–5 kHz), oscillations in the dipolar order have been observed in polyoxymethylene (Veeman 1979).

In equilibrium at ambient temperature, the dipolar reservoir is essentially disordered. However, the cross-polarization process, used to provide carbon magnetization (figure 1), produces

Downloaded from rsta.royalsocietypublishing.org

substantial dipolar ordering at a temperature not too different from that of the carbon rotating frame reservoir (VanderHart & Garroway 1979; Garroway *et al.* 1979*b*). The mechanism is the following: just after the spin-lock pulse is applied to the protons, a transient oscillation (Strombotne & Hahn 1964) ensues between the proton rotating frame Zeeman reservoir and the proton rotating frame dipolar reservoir. This oscillation damps out in a time determined by proton spin fluctuations, leaving a fraction of the initial polarization in the rotating frame dipolar reservoir.

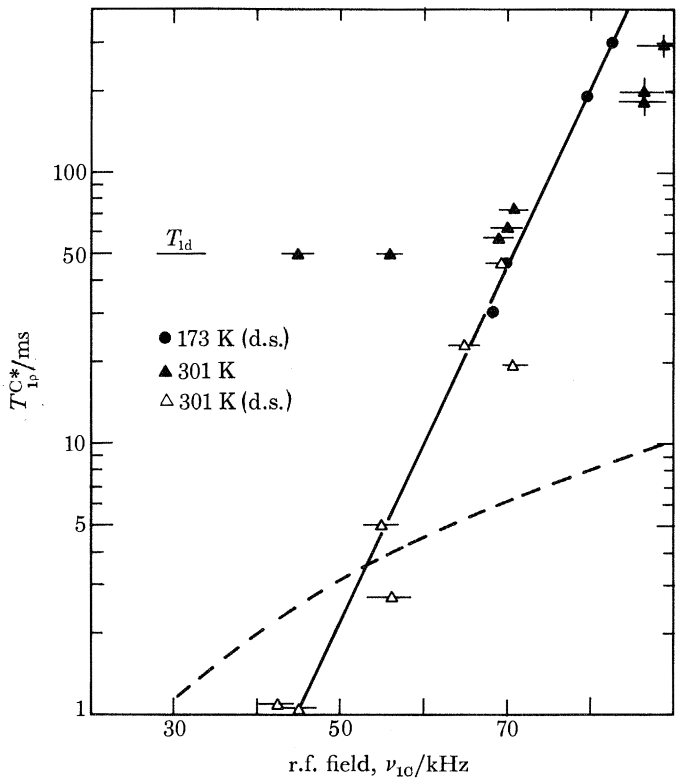

FIGURE 3. The r.f. field dependence and temperature dependence of the *observed* ^{13}C rotating frame relaxation time $T^{C*}_{1\rho}$, adapted from VanderHart & Garroway (1979). The static sample of ultra-orientated polyethylene (u.o.p.e.) is aligned with draw axis parallel to B_0. At 173 and 301 K the values of T_{1d} is 50 ms as shown. For low r.f. field strengths the effective relaxation time is nearly T_{1d}. When dipolar order is suppressed (d.s.), the early relaxation time becomes T^{d}_{CH} (cf. figure 1). Except above 80 kHz at 301 K, the d.s. data are well fitted by an exponential r.f. field dependence with correlation time $\tau_d = 24$ μs (solid curve). The broken line represents a square law r.f. field dependence, arbitrarily scaled.

When the proton r.f. field is removed, the rotating frame dipolar order is instantly converted into laboratory frame dipolar order. For proton r.f. fields satisfying $\omega^2_{1H} \gg M^{(2)}_{HH}$, where $M^{(2)}_{HH}$ is the truncated proton–proton second moment and $\omega_{1H} = \gamma_H B_{1H}$, then the inverse temperature β_d of the dipolar reservoir is related to the initial inverse temperature $\beta_H(0)$ of the proton rotating frame reservoir by $\beta_d \approx \frac{3}{4}\beta_H(0)$. During cross-polarization, the proton and carbon r.f. fields are matched to $\omega_{1C} = \omega_{1H}$, and after a sufficient time the carbon system reaches an inverse temperature of $\beta_C \approx \beta_H(0)\,(1 - M^{(2)}_{HH}/4\omega^2_{1H})$; the fraction in parentheses accounts for the proton spin polarization lost during the proton transient oscillation. Hence in the carbon $T^C_{1\rho}$ experiment, when the proton r.f. field is turned off (just after cross-polarization, figure 1), the carbon rotating frame and proton dipolar reservoirs are already at rather similar temperatures and so the spin–

Downloaded from rsta.royalsocietypublishing.org

spin pathway via T_{CH}^{d} will not be so important provided the dipolar reservoir is not rapidly depleted into the lattice.

The competition of spin–lattice and spin–spin pathways has been illustrated in a study (VanderHart & Garroway 1979) on ultra-orientated polyethylene, a material in which the spin–spin effects predominate at room temperature. This system was chosen as a reasonably tractable spin system with substantial carbon–proton dipolar coupling. Here spin–spin effects predominate primarily because the backbone reorientation in polyethylene is slow and modulates only a small fraction of $M_{CH}^{(2)}$.

The dependence of the observed rotating frame decay time $T_{1\rho}^{C*}$ on r.f. field strength is shown in figure 3 for ultra-orientated polyethylene (u.o.p.e.) with the draw axis (and hence the chain axes) along B_0. In a modification of the $T_{1\rho}$ experiment, two r.f. pulses, separated by a time somewhat longer than the proton T_2, were applied to the protons just after cross-polarization. The r.f. pulse duration was selected to cause a nutation of 54.7°. These two magic angle pulses suppress any proton dipolar order to less than 3 % of its initial value. In figure 3, those data for $T_{1\rho}^{C*}$ with dipolar suppression are denoted by d.s. Clearly if $T_{1\rho}^{C*}$ actually represents a purely motional relaxation, then the status of the proton dipolar spin system will be irrelevant. Further, for slow motion, one expects no greater than a ν_{1C}^{2} field dependence, shown as a broken line. (By convention we report r.f. field strength in hertz: $\nu_{1C} = \omega_{1C}/2\pi$.) This observed behaviour of $T_{1\rho}^{C*}$ is explained by the reservoir picture in figure 2. For r.f. fields below about 70 kHz, T_{CH}^{d} is less than T_{1d}. When the proton field is removed just after the carbon–proton cross-polarization, the carbon reservoir is at essentially the same temperature as the dipolar system, as predicted above; the carbon and dipolar reservoirs are in good thermal contact and the carbon magnetization is dragged down by the dipolar reservoir with decay time T_{1d}, here 50 ms at 301 K. When the dipolar order is suppressed, however, the dipolar reservoir appears as a highly disordered, large, but not infinite, sink and so the early carbon relaxation time is given directly by T_{CH}^{d} for experiment d.s. Above about 70 kHz, the carbon magnetization is less strongly coupled to the dipolar system and cannot follow the dipolar decay; here $T_{1\rho}^{C*}$ is determined by T_{CH}^{d}.

From the r.f. field dependence of the spin–spin relaxation time T_{CH}^{d}, a value of 24 μs is inferred for the dipolar fluctuation time, in good agreement with the calculated rigid lattice value of 24.2 ± 1.2 μs. At the very highest r.f. fields the $T_{1\rho}^{C*}$ values at 301 K deviate from the exponential field dependence in figure 3; these data points may reflect some motional contributions. From the $T_{1\rho}^{C*} = 36$ ms datum at 373 K and 87 kHz (not shown), a motional correlation time of 7 ± 0.5 μs is found, which agrees with $\tau_C \approx 4$ μs from proton relaxation data (McCall & Douglass 1965).

Figure 4 illustrates one of the hazards of these spin–spin effects. Shown are the carbon rotating frame magnetization decay curves for 'regular' and 'short' specimens of u.o.p.e. at 173 K. The regular sample is a cylinder slightly taller than the carbon solenoidal r.f. coil; the short sample is barely over one-half as tall and of the same diameter. The non-exponential behaviour over the first 5–10 ms arises from those spins in weaker carbon r.f. fields that then have a much shorter spin–spin relaxation time. The different decay rates beyond 10 ms are due to the difference in r.f. field strengths (83 kHz for the regular sample and 80 kHz for the short sample). At 173 K, u.o.p.e. is an extreme example in which there is very little molecular motion to compete with spin–spin processes; here the non-exponential decay relates only to the r.f. coil inhomogeneity rather than to any intrinsic properties of the specimen.

For the polyethylene, only data at the highest r.f. field (87 kHz) and high temperature (373 K) clearly reflect molecular motion. Similarly, in the crystalline region of polyoxymethylene, the

PHILOSOPHICAL TRANSACTIONS OF THE ROYAL SOCIETY A MATHEMATICAL, PHYSICAL & ENGINEERING SCIENCES

PHILOSOPHICAL TRANSACTIONS OF THE ROYAL SOCIETY A MATHEMATICAL, PHYSICAL & ENGINEERING SCIENCES

Downloaded from rsta.royalsocietypublishing.org

rotating frame relaxation is found to be dominated by spin–spin effects (Veeman *et al.* 1979; Stejskal *et al.* 1979).

In disordered organic glasses the situation is more favourable. From examination of the r.f. field dependence of $T_{1\rho}^{C*}$ in an epoxy polymer, Garroway *et al.* (1979*b*) showed that the observed relaxation times are dominated by molecular motions for r.f. fields above 40 kHz. Schaefer, Stejskal and coworkers have concluded by direct comparison of $T_{1\rho}^{C*}$ with T_{CH}^{d} (non-spinning) and by the r.f. field dependence of $T_{1\rho}^{C*}$ that for a wide variety of glassy engineering polymers (polystyrene, polymethylmethacrylate, dimethylphenylene oxide, polycarbonate and polyethylene terephthalate) studied at room temperature, the spin–spin effects are small, though they account for the order of 10–20 % of the relaxation rate at an r.f. field strength of 30–40 kHz (Stejskal *et al.* 1979; Schaefer *et al.* 1980).

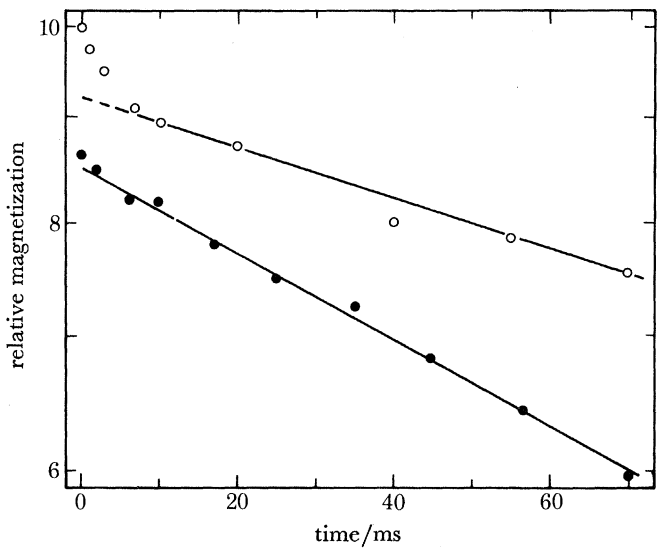

FIGURE 4. Comparison of the decay of ^{13}C spin-lock magnetization for 'regular' (○) and 'short' (●) u.o.p.e. samples at 173 K, from VanderHart & Garroway (1979). R.f. field strengths are 83 and 80 kHz, respectively. The magnetizations have been displaced vertically for clarity. The initial decay for the regular specimen over the first 5–10 ms arises from those spins at the ends of the sample that see a smaller r.f. field because of coil inhomogeneity and consequently decay more rapidly to the dipolar reservoir.

This simplified summary of the complications of spin–spin effects bypasses some of the problems in interpretation of rotating frame relaxation. Whatever the drawbacks of proton–proton spin diffusion, its effect is to produce a nominal average over different environments. That is not so for carbon relaxation. One expects an orientation dependence of $T_{1\rho}^{C}$ if the spin–lattice relaxation is dominated by only a few, perhaps directly bonded, protons. Any orientation dependence is partly averaged by the sample spinning. Furthermore, in amorphous polymer systems at ambient temperature, the heterogeneous environments may lead to distributions of motional behaviour. The difficulty centres on the extraction of such distributions from a non-exponential decay of resonance signals, which, by nature, are rather weak and can only be monitored over a decay of, say, one decade. Accordingly, it is our feeling that spin–spin effects should be reduced as much as possible, by large r.f. fields or elevated temperature, wherever practical, so that spin–spin effects can be dismissed out of hand in any comprehensive analysis of motional relaxation in solids. (Of

Downloaded from rsta.royalsocietypublishing.org

course, rapid molecular motion may affect the cross-polarization rate so that not all spins are properly counted.)

(*b*) *Phase noise and relaxation*

As a second example of rotating frame relaxation not due to motion, we consider phase noise in the (carbon) r.f. transmitter.

The spectrum of any frequency source is not perfectly pure. In general the jumps in the r.f. phase are small (r.m.s. deviation less than 1 rad) and the duration of the jump is rapid, so that the weak collision approximation is valid. By comparison, amplitude noise may be generally ignored (Meyer 1970; Shoaf *et al.* 1973). A randomly varying phase may be represented as an instantaneous variation $\Delta\omega_0(t)$ in the carrier frequency so that in the rotating frame the r.f. field Hamiltonian is, for nominally resonant irradiation,

$$\mathscr{H} = \omega_1 S_x + \Delta\omega_0(t) S_z, \tag{6}$$

where S_x, S_z are the spin operators along the r.f. and B_0 directions, respectively. In contrast to the $T_{\mathrm{CH}}^{\mathrm{d}}$ mechanism, for which (carbon) spins see fluctuating carbon–proton dipolar fields that are essentially uncorrelated, here all the spins see the *identical* fluctuation $\Delta\omega_0(t)$. Very slow fluctuations will be followed adiabatically by the spin-locked magnetization; very fast fluctuations occur too rapidly to allow substantial dephasing of the magnetization. The important fluctuations in $\Delta\omega_0$ are those at ω_1, and the effective relaxation time $T_{1\rho}^{\phi}$ due to these phase fluctuations at the spin-lock frequency is then

$$(T_{1\rho}^{\phi})^{-1} = S_{\Delta\omega}(\omega_1) = (2\pi)^{-1}\Delta\omega^2 J_{\Delta\omega}(\omega_1), \tag{7}$$

where the fluctuations $\Delta\omega_0(t)$ are described by $S_{\Delta\omega}(\omega)$, the spectral density of *frequency* fluctuations at ω. The total mean squared frequency deviation over the entire spectrum is

$$\Delta\omega^2 = \int_{-\infty}^{\infty} \mathrm{d}\omega\, S_{\Delta\omega}(\omega), \tag{8}$$

and $J_{\Delta\omega}(\omega)$ is the normalized spectral density, namely $\int_{-\infty}^{\infty} \mathrm{d}\omega\, J_{\Delta\omega}(\omega) = 2\pi$. (The functions $S_{\Delta\omega}(\omega)$ and $J_{\Delta\omega}(\omega)$ are two-sided transforms, e.g. $S_{\Delta\omega}(-\omega) = S_{\Delta\omega}(\omega)$, in contrast to the single-sided transforms of Shoaf *et al.* (1973).)

Frequency synthesizer phase noise is generally specified by the single sideband noise power density (per hertz) $\mathscr{L}(\nu)$ (Meyer 1970; Shoaf *et al.* 1973). For small phase fluctuations this is identical to the spectral density of *phase* fluctuations and is related to the density $S'_{\Delta\omega}(\nu)$ for *frequency* fluctuations:

$$\mathscr{L}(\nu) = S'_{\Delta\phi}(\nu) = \omega^{-2} S'_{\Delta\omega}(\nu), \tag{9}$$

where $S'_{\Delta\phi}(\nu)$ and $S'_{\Delta\omega}(\nu)$ are the Fourier transforms of the autocorrelation functions for phase and frequency, respectively, and the frequency argument is in hertz. The frequency argument is changed to radians by $S'_{\Delta\omega}(\nu) = 2\pi S_{\Delta\omega}(\omega)$ and so (7) becomes

$$(T_{1\rho}^{\phi})^{-1} = 2\pi\nu_1^2 \mathscr{L}(\nu_1). \tag{10}$$

In a typical synthesizer-driven spectrometer the power level of the synthesizer is so high (about 10 dBm) that the *random* noise introduced by later transmitter amplification stages is negligible and only synthesizer noise need be considered. Within a few kilohertz from the carrier frequency the phase noise power $\mathscr{L}(\nu)$ falls off as ν^{-1}. For this flicker noise approximation, the phase noise relaxation rate (equation (10)) increases linearly with r.f. field strength ν_1 and the dependence very gradually approaches a quadratic as white noise dominates. For a typical 160 MHz

Downloaded from rsta.royalsocietypublishing.org

synthesizer (Rockland Model 5600†) the (non-spurious) phase noise $\mathscr{L}(\nu)$ is specified to be less than -125 dB relative to the carrier power at 100 kHz from the carrier frequency. For a carbon r.f. field strength of $\nu_{1C} = 100$ kHz, (10) predicts the phase noise relaxation time to be $T_{1\rho}^{\phi} = 50$ s, for a spectrometer in which the synthesizer frequency directly determines the transmitter frequency. For comparison, in a cured epoxy at room temperature, values of $T_{1\rho}^{C}$ range from 10 to 60 ms at a field strength of 66 kHz (Garroway *et al.* 1979*a*). In u.o.p.e. at 373 K, $T_{1\rho}^{C} = 36$ ms for the crystalline region (VanderHart & Garroway 1979). If the synthesizer is used to provide an intermediate frequency, the phase noise relaxation rate will increase accordingly.

3. Spectral resolution

Carbon line widths in organic solids are generally broader than in liquids. We are concerned here with the likely origins of the broadening mechanisms in solids: can one expect better resolution in the near future by modest improvements in the present techniques? If these limitations are imposed by the specimen itself, can further information about the specimen be extracted from the observed line widths?

(*a*) *Decoupling efficiency*

For a heteronuclear spin system, efficient decoupling of the protons is closely related but not identical to the maintenance of a spin-locked carbon state. Both spin–spin and spin–lattice effects play a role.

(i) *Spin–lattice effects*

The coherent proton decoupling used in these experiments relies on averaging to zero the heteronuclear dipolar interaction $I_z S_z$ with a periodicity of $\nu_{1H}^{-1} = (\omega_{1H}/2\pi)^{-1} = (-\gamma_H B_{1H}/2\pi)^{-1}$, where B_{1H} is the proton decoupler r.f. field strength. Those fluctuations in $I_z S_z$ with frequencies at ω_{1H}, in particular molecular fluctuations, will weaken the averaging process. The carbon rotating frame spin–lattice relaxation time $T_{1\rho}^{C}$ monitors the same motions in the $I_z S_z$ term but responds to fluctuations at ω_{1C}. For $\omega_{1H} = \omega_{1C}$, the relaxation time T_{2m}, associated with the line width due to this modulation, is simply related to $T_{1\rho}^{C}$ (Garroway *et al.* 1979*a*, *b*; VanderHart *et al.* 1981):

$$T_{2m}(\omega) = T_{1\rho}^{C}(\omega). \tag{11}$$

Hence $T_{1\rho}^{C}$ provides an estimate of the lifetime broadening of the resonantly decoupled spectral lines. In an epoxy polymer the contribution to the line width from this mechanism is found to be not greater than 35 % for the seven resolved spectral lines at room temperature and for a decoupling field strength of 66 kHz (Garroway *et al.* 1979*a*). At lower temperature, $T_{1\rho}^{C}$ for the methyl carbons decreases as the methyl reorientation slows down; the methyl resonance broadens and finally disappears at about 151 K. The temperature dependence of this epoxy spectrum is shown and further discussed in §3*e*.

(ii) *Spin–spin effects*

For a proton decoupling field that is off-resonance, a fraction of the $I_z S_z$ dipolar interaction is not averaged to zero during decoupling (Bloch 1958). However, proton–proton spin fluctuations

† Reference to a company or product name does not imply approval or recommendation by any agency of the U.S. Government of the product or services to the exclusion of others that may be suitable.

Downloaded from rsta.royalsocietypublishing.org

will further reduce this residual component by 'self-decoupling', with an efficiency that depends on the orientation of the effective r.f. field and B_0. For small deviations from resonance, the broadening for off-resonant proton irradiation (Mehring 1976) may be written (VanderHart *et al.* 1981)

$$\Delta\nu_{\text{o.r.p.i.}} = \pi^{-\frac{1}{2}} (\Delta\omega_{0\text{H}}/\omega_{1\text{H}})^2 M_{\text{CH}}^{(2)} \tau_{\text{d}}, \tag{12}$$

where $\Delta\omega_{0\text{H}}$ is the proton resonance offset, $\omega_{1\text{H}}$ is the decoupling field strength and $M_{\text{CH}}^{(2)}$ and τ_{d} are the carbon–proton second moment and dipolar fluctuation time introduced earlier. In this approximation the r.f. decoupling and self-decoupling act together; narrower lines will occur for protonated carbons with *strong* proton–proton coupling than for isolated protons directly bonded to the carbons.

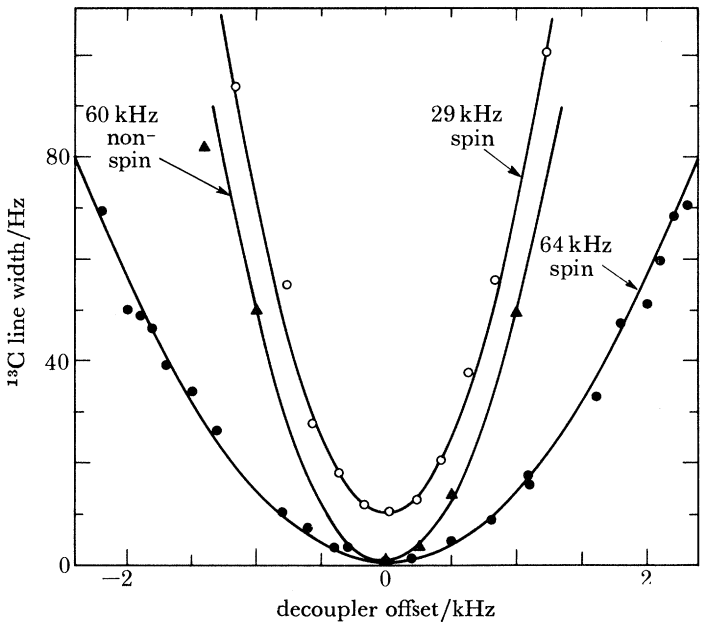

FIGURE 5. ^{13}C line width (full width at half height) for spinning and static u.o.p.e. specimens at room temperature, adapted from VanderHart *et al.* (1981). The draw axis and hence chain axes are parallel to B_0 for the static sample and parallel to the magic angle rotation axis for the spinning sample. R.f. field strengths are indicated; the indirect determination of line width for the static sample is described in the text.

Equation (12) should be reinterpreted for sample spinning. Rapid rotation at the magic angle at a rotational speed Ω_{rot} leads to an increase in τ_{d} when spinning speed approaches the proton–proton coupling strength. Further, owing to proton chemical shift anisotropy, the proton resonance becomes a periodic function of the spinning rate, and so the protons will generally be irradiated off resonance. Since the line width depends quadratically on proton resonance offset, this line width contribution cannot average to zero over the rotational period. For a single crystal with closely spaced proton resonance frequencies, this off-resonance contribution may be smaller in a static sample than in one that is spun.

For unknown organic specimens one must allow for irradiating protons perhaps $\pm 4 \times 10^{-6}$ off resonance. For a singly protonated carbon with $\tau_{\text{d}} = 25$–$60\,\mu\text{s}$ and a powder averaged second moment of $M_{\text{CH}}^{(2)} = 4.4 \times 10^9\,\text{rad}^2/\text{s}^2$, (12) leads to a broadening of 1–2.5 Hz (0.07–0.17×10^{-6}) for an r.f. field of 60 kHz and static field of 1.4 T (VanderHart *et al.* 1981). This effect worsens at high static field where, in addition, high r.f. fields are more difficult to produce; for an r.f. field of

Downloaded from rsta.royalsocietypublishing.org

40 kHz and $B_0 = 4.7\ T$, then the off-resonance line width contribution is 25–60 Hz ($0.5–1.2 \times 10^{-6}$). Furthermore, if high magic angle spinning speeds (5–8 kHz) are routinely achieved for high field applications, the self-decoupling effect will be moderated, through the increase in τ_d, leading to broader peaks.

Figure 5 shows the increase in ^{13}C line width on moving away from proton resonance for a specimen of ultra-orientated polyethylene (u.o.p.e.), under both spinning and non-spinning conditions (VanderHart *et al.* 1981). The draw axis is aligned parallel to the magic angle spinning axis or, for the static sample, parallel to B_0. The data are for the resonance associated primarily with the crystalline regions. To reduce other sources of broadening, the line widths have been determined from ^{13}C T_2 values from a spin-echo sequence. For the spinning experiment the echo sequence was rotationally synchronized (Earl & VanderHart 1979). For the static specimen, line width was measured indirectly. The crystalline signal was enhanced, relative to the amorphous signal, by preparing the carbon magnetization by cross-polarization from a state of dipolar order. The carbon r.f. field was then lowered to only 1.0 kHz while the protons were simultaneously decoupled at 60 kHz. In this 'decoupled $T_{1\rho}^C$' experiment the rotating frame carbon magnetization is insensitive to any ^{13}C–^{13}C dipolar coupling, while the enormous r.f. field mismatch minimizes carbon–proton cross-polarization. For the non-spinning results the quoted line widths are determined by $(\pi T_{1\rho}^C)^{-1}$, where the rotating frame relaxation is measured under the described decoupling conditions. On resonance, $T_{1\rho}^C = 450$ ms is found and corresponds to a line width of 0.7 Hz.

For the static sample the dipolar fluctuation time is directly available from the r.f. field dependence of T_{CH}^d (equations (3) and (4) and figure 3). With the value $\tau_d = 24\ \mu s$ and with (12), the off-resonance proton irradiation data of figure 5 predict a carbon–proton second moment that is a factor of 1.37 larger than the moment calculated for a C–H bond distance of 0.109 nm (VanderHart *et al.* 1981). Agreement, though reasonable, is not exact.

For the spinning specimen the correlation time $\langle \tau_d \rangle_r$, averaged over the rotation, may be inferred from the data by aid of the assumption that $\langle M_{CH}^{(2)} \tau_d \rangle_r \approx \langle M_{CH}^{(2)} \rangle_r \langle \tau_d \rangle_r$. For the two r.f. fields of 29 and 64 kHz the values 16.8 and 18.4 μs are found. This difference is not considered significant. The spin–spin correlation time is substantially shorter in the spinning than in the non-spinning specimens; in the latter, for the draw axis (and, to a great extent, the chain axes) parallel to B_0, the proton spin exchange *within* a methylene group does not produce a fluctuating field at that methylene carbon nucleus since the methylene protons are equivalent at this orientation. In this respect u.o.p.e. aligned along B_0 does not present an anomalously strongly coupled spin system: polycrystalline polyethylene is more strongly coupled (VanderHart & Garroway 1979).

Even for proton decoupling that is precisely on resonance, there may be a carbon–proton dipolar line width contribution if the r.f. field ω_{1H} is inadequate. The spin–spin relaxation that determines the line width corresponds to the cross-polarization time between carbon and proton rotating frame reservoirs in the limit where ω_{1C} approaches zero (Demco *et al.* 1975; Mehring 1976; Garroway *et al.* 1979*b*; VanderHart *et al.* 1981). The line width $\Delta\nu_{i.d.p.}$ due to inadequate decoupling power (i.d.p.) is

$$\begin{aligned} \Delta\nu_{i.d.p.} &= (2\pi)^{-1} M_{CH}^{(2)} J_{s.l.}(\omega_{1H}) \\ &= (4\pi)^{-\frac{1}{2}} M_{CH}^{(2)} \tau_{s.l.} \exp -(\tfrac{1}{4}\omega_{1H}^2 \tau_{s.l.}^2), \end{aligned} \tag{13}$$

where a Gaussian correlation function with correlation time $\tau_{s.l.}$ is assumed to describe the spin–spin fluctuations under spin-lock (s.l.) conditions at large ω_{1H} (Mehring 1976). Because of

Downloaded from rsta.royalsocietypublishing.org

the strong r.f. field dependence, it is easy to ensure that this contribution is quite negligible once a threshold is overcome. For both polycrystalline and ultra-orientated polyethylene, no decrease in line width is found above a decoupling field of 40 kHz (VanderHart *et al.* 1981). The residual homogeneous widths in the spinning experiment for polycrystalline (not shown) and ultra-orientated polyethylene are 1.5 and 1.0 Hz, respectively, at 64 kHz decoupling field. The off-resonance effect due to proton chemical shift anisotropy can account for only 0.05 Hz and the magnitude of this 1 Hz width is not presently understood. Further, from the r.f. field dependence of the line width at low field strength, VanderHart *et al.* (1981) extract a correlation time $\langle\tau_{\mathrm{s.l.}}\rangle$ that is approximately 30 % longer than predicted by the rotationally averaged version of the expression for $\tau_{\mathrm{s.l.}}$ (Mehring 1976), which, however, applies in the large r.f. field limit. If this discrepancy is real, it indicates that some mechanism is reducing the efficiency of the self-decoupling mechanism.

(*b*) *Magic angle spinning*

Rotor instability and inaccuracy in setting the magic angle degrade the line width, but these are technical problems, extrinsic to the specimen. A more interesting aspect is the influence of molecular motion on the averaging process of magic angle spinning (Maricq & Waugh 1979; Suwelack *et al.* 1980). Though there are subtle features when the mechanical rotation period approaches the molecular jump time of the chemical shift anisotropy tensor, the main impact of molecular motion is to reduce the averaging efficiency according to (VanderHart *et al.* 1981)

$$\Delta\nu_\sigma \equiv (\pi T_{2\sigma})^{-1} = \pi^{-1}\langle M_\sigma^{(2)}\rangle_{\mathrm{m}}\tau_{\mathrm{c}}/(1+\Omega_{\mathrm{rot}}^2\tau_{\mathrm{c}}^2), \tag{14}$$

where $\Delta\nu_\sigma$ is the excess line width, associated with a relaxation time $T_{2\sigma}$, due to motional modulation of the chemical shift anisotropy tensor. It is presumed here that the isotropic shift is unaffected. The second moment of the chemical shift anisotropy modulated by the motion is $\langle M_\sigma^{(2)}\rangle_{\mathrm{m}}$ and τ_{c} is the molecular correlation time. Isotropic reorientation is a limiting case. For aliphatic carbons (*ca.* 30×10^{-6} anisotropy) and aromatic, carboxyl, carbonyl or vinyl carbons (*ca.* 150×10^{-6} anisotropy), one expects a maximum line width (at $\Omega_{\mathrm{rot}}\tau_{\mathrm{c}}=1$) of 7 and 180 Hz (0.5 and 12×10^{-6}), respectively, for $B_0 = 1.4$ T and a spinning speed of 2.5 kHz. At higher field (4.7 T with only 5 kHz spinning speed) this worsens to 40 and 1000 Hz (0.8 and 20×10^{-6}), respectively. For highly anisotropic motion this problem is lessened and can in principle be avoided by selecting a more felicitous temperature.

This broadening from the modulation of the anisotropic chemical shift is sensitive to slow motions, of the order of Ω_{rot}. On the other hand, in the carbon spin-locking experiment the rotating frame magnetization is relaxed as well by a fluctuating chemical shift tensor, but there the sensitivity is to fluctuations at $\omega_{1\mathrm{C}}$. Detailed comparison of the carbon line width and $T_{1\rho}^{\mathrm{C}*}$ and their respective dependences on Ω_{rot} and $\omega_{1\mathrm{C}}$ will isolate this contribution.

(*c*) *Phase noise broadening*

The destruction of rotating frame magnetization by synthesizer phase noise, considered in §2*b*, is intimately related to the more usual question of the degradation and line broadening of the detected signal in a homodyne receiver in which a noisy synthesizer is used to phase detect the n.m.r. signal. In this latter case random *phase* fluctuations are important at the frequency of the demodulated line, i.e. at the carbon resonance offset frequency. By the ν^{-1} nature of the flicker phase noise, the most severe noise is close to the carrier frequency. At 1 Hz from resonance the single sideband phase noise per hertz band width is about -80 dB for a typical synthesizer

PHILOSOPHICAL TRANSACTIONS OF THE ROYAL SOCIETY A MATHEMATICAL, PHYSICAL & ENGINEERING SCIENCES

PHILOSOPHICAL TRANSACTIONS OF THE ROYAL SOCIETY A MATHEMATICAL, PHYSICAL & ENGINEERING SCIENCES

Downloaded from rsta.royalsocietypublishing.org

(Rockland 5600), leading to a deterioration of 10^{-4} in the (voltage) signal:noise ratio of a quadrature detected 1 Hz wide peak. This is not currently a limitation in solid state spectrometers.

(*d*) *Susceptibility*

For an ellipsoidal specimen of macroscopically homogeneous material with isotropic susceptibility χ placed in an (initially) uniform magnetic field, the magnetic field within is also uniform. This idealization does not pertain to the magic angle spinning geometry. There a crushed powder perhaps with anisotropic bulk susceptibility is compressed to an arbitrary degree into a spinner of low symmetry. Nearby, producing irregular fields, are the spinner's stator or axle support system. Indeed, just the geometry of the spinner assumbly can introduce serious (1×10^{-6}) line broadening, as may be verified by observing a motionally narrowed liquid in a magic angle sample spinning apparatus for which the static field has been shimmed in the absence of the spinner assembly.

In a powdered sample in which the bulk susceptibility is small, the magnetic field variation with a particular particle may be decomposed into contributions from the internal demagnetization field of that particle and from the external fields of all other particles. For a prolate spheroid embedded in an array of closely packed *spheres*, Drain (1962) estimates a line width (defined as twice the root of the second moment) of $3\chi B_0$, where the susceptibility is assumed to be isotropic. For organic powders, without magic angle spinning, this leads to a susceptibility broadening on the order of 1×10^{-6}. In a static sample of adamantane, T. Terao (personal communication, 1979; Terao *et al.* 1981) finds that the ^{13}C line width is reduced from 47 to 28 Hz (a change of 1.3×10^{-6} at 1.4 T) on compression at above 5 MPa into a sphere; presumably this compaction removes most of the voids. He finds similar reduction on dispersing the powder in C_6H_6 and CCl_4.

Under magic angle spinning, some of these broadening effects will disappear for local field variations that transform as $P_2(\cos\theta)$. The line broadening from the external fields of spherical particles (of isotropic susceptibility) vanishes under magic angle spinning (Doskočilová *et al.* 1975). In general, magic angle spinning should remove susceptibility broadening in a powder of *arbitrarily* shaped particles confined in a chamber of arbitrary shape, provided that the various susceptibilities are both small and isotropic (VanderHart *et al.* 1981). This may be seen by approximating a particle in the static magnetic field by a collection of small, uniformly polarized spheres. Nuclei within a sphere see a superposition of the Lorentz field, $\frac{4}{3}\pi\chi B_0$, and the dipolar fields from all the other spheres. This latter contribution is then removed by magic angle spinning. Spinning also removes some of the broadening arising from the non-ellipsoidal geometry of the spinner assembly, and adjustment of the shim coils may compensate for some of the higher-order harmonics.

The bulk susceptibility tensor may be anisotropic; one example is hexamethylbenzene with $\chi_\parallel - \chi_\perp = -0.405 \times 10^{-6}$ (Landolt-Börnstein 1967). In a polycrystalline powder the local magnetic field in one crystallite is determined by the orientation of the susceptibility tensors in the nearby crystallites and magic angle spinning will not completely remove the broadening due to the random distribution of the orientations of the susceptibility tensors. Anisotropic susceptibility broadening is analogous to chemical shift screening by nearby ring currents (VanderHart *et al.* 1981); the isotropic average of the ring current shift is non-zero. Spherical single crystal studies then become attractive to remove these problems of anisotropic susceptibility.

For hexamethylbenzene, when the magic angle is critically set, the methyl and aromatic line widths are equal and generally greater than magnet inhomogeneity. At 1.4 T, VanderHart *et al.*

Downloaded from rsta.royalsocietypublishing.org

(1981) observed a 15 Hz line width, of which 4 Hz represents magnet inhomogeneity and drift; at 4.7 T the lines were 50 Hz wide with less than 1 Hz of magnet inhomogeneity. The excess line width of $0.7–0.9 \times 10^{-6}$ is attributed to the bulk anisotropic susceptibility in hexamethylbenzene, in support of the observation by M. Alla (personal communication, 1978) that the ^{13}C methyl line width in hexamethylbenzene increases approximately with static field, in contrast to line widths for adamantane.

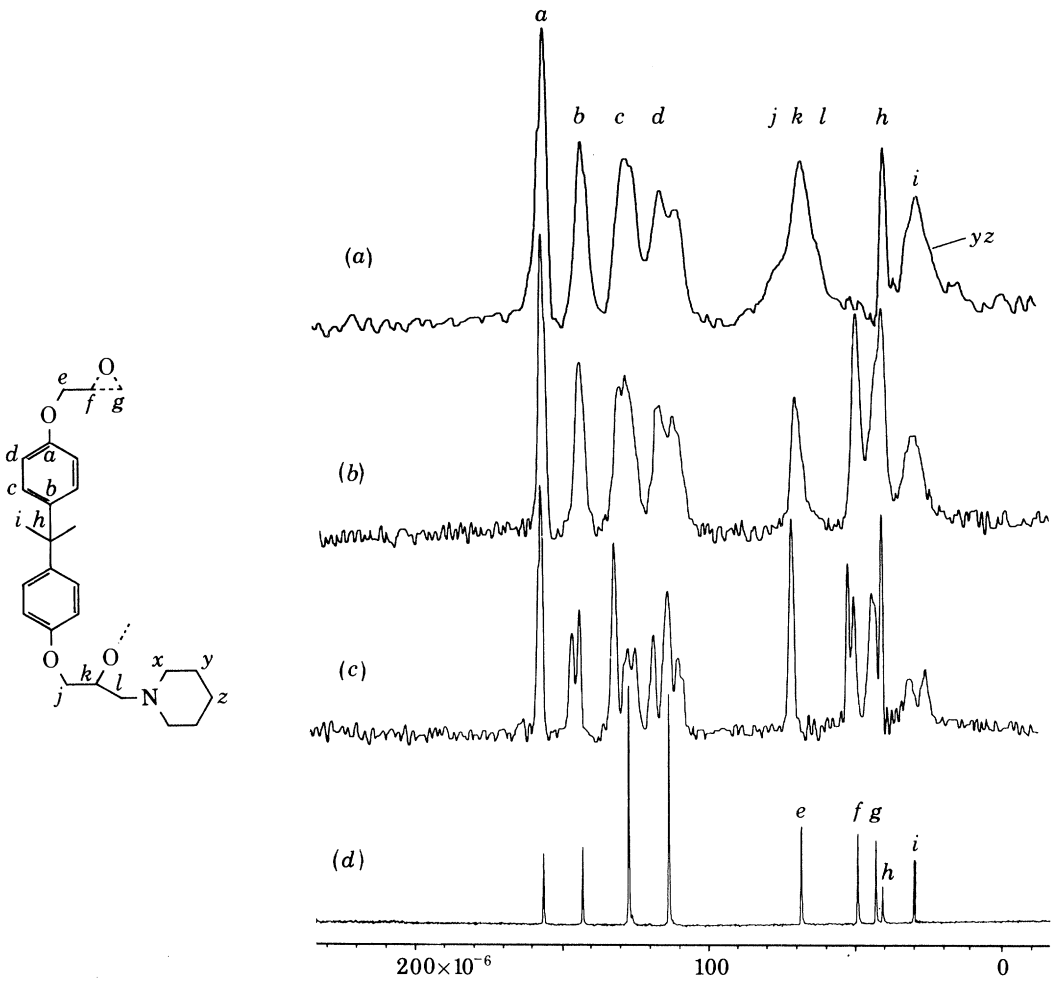

FIGURE 6. ^{13}C spectra of the epoxy resin diglycidyl ether of bisphenol A (DGEBA) in four different phases: (*a*) polymerized with 5 % by mass of piperidine, 247 K; (*b*) amorphous resin, 230 K; (*c*) polycrystalline resin, 230 K; (*d*) in CCl_4, solvent peak deleted. The chemical structure on the left shows one half of the (symmetrical) monomer in the top half and a possible curing structure with piperidine (bottom half) in the aromatic region. In the amorphous phase much of this detail is smoothed out, presumably by the distribution of molecular environments leading to a distribution of *isotropic* chemical shifts. The spectra of amorphous and polymerized phases are quite similar in the aromatic region.

(*e*) *Distribution of isotropic chemical shifts*

Figure 6 compares spectra for different phases of an epoxy resin, diglycidyl ether of bisphenol A (DGEBA). As a pure monomer (Dow DER 332) the resin crystallizes with a melting temperature of 315.5 ± 0.5 K; its spectrum is shown here at 230 K. The polycrystalline resin was then melted and supercooled to 230 K to produce an amorphous phase. Also shown are the spectra of

Downloaded from rsta.royalsocietypublishing.org

the polymerized monomer, cured with 5 % by mass of piperidine, and the liquid-state spectrum of the starting resin. (This latter spectrum was obtained on a liquid-state spectrometer and the CCl_4 solvent peak has been deleted.) The top half of the indicated chemical structure represents one-half of the unreacted epoxy monomer, while a possible curing structure with the piperidine is represented in the lower half.

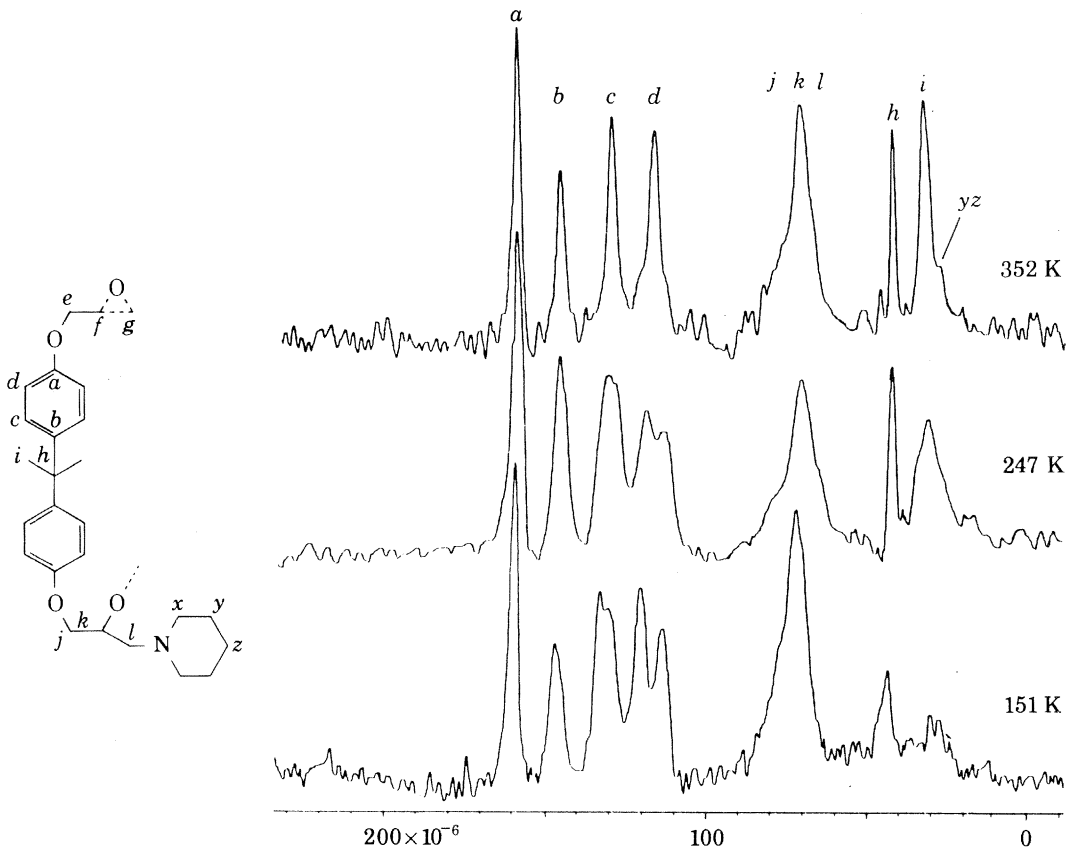

FIGURE 7. The ^{13}C spectra over a 200 K temperature range for DGEBA epoxy cured with piperidine. The chemical structure on the left shows one half of the (symmetrical) monomer (top half) and a possible curing structure with piperidine (bottom half). In the spectra the methyl resonance broadens and then disappears at low temperature; the remaining peak at about 25×10^{-6} is assigned to the piperidine. The low-temperature splittings of peaks *c* and *d* collapse at higher temperature, indicating reorientation of the phenyl group with respect to the backbone.

In comparison with the liquid-state spectrum, the crystalline-state resin spectrum of figure 6 is far more complex; the splittings of the main peaks represent magnetically inequivalent rigid carbons that become equivalent in the liquid. The connection between the crystalline spectrum and the X-ray determined crystal structure will be presented elsewhere (Garroway *et al.* 1981). Salient features are the splitting of the methyl peak by 5.0×10^{-6}; as discussed below, these peaks are wide at this temperature but are quite well resolved at ambient temperature. For the protonated aromatic carbons, three and four lines are resolved in the crystalline phase.

In the amorphous-state spectrum of figure 6 much of this structural detail is smoothed out, though two peaks are just resolved for each of the protonated aromatic carbons. For the polymerized specimen the opening of the epoxide groups has shifted the two epoxide resonances

Downloaded from rsta.royalsocietypublishing.org

downfield, where they overlap with the methylene resonance (Garroway *et al.* 1976), yet the aromatic peaks are virtually identical in the amorphous and polymerized phases.

In the crystalline phase many of the carbons within the unit cell are inequivalent. The narrow lines arise from the extreme regularity of the crystalline environment. In this spectrum, with the exception of the methyl resonances, most of the line broadening is probably attributable to magnet inhomogeneity, magic angle imperfections and susceptibility effects.

The distribution of local molecular environments in the amorphous phase blurs out the sharp detail of the crystalline-state spectrum. Polymerization freezes the molecules into a random distribution of orientations which, based on these spectra, is apparently not too different from the distribution in the glassy state of the neat resin.

Further evidence of a distribution of isotropic chemical shifts is also found in the temperature dependence over 200 K of the epoxy polymer spectrum (figure 7). At low temperature (151 K) peak *d* assigned to the aromatic carbon *ortho* to the oxygen is resolved into two, with a splitting of 8×10^{-6}; line *c* for the carbon *meta* to the oxygen is rather broad but a trace of two peaks is seen, separated by about 3×10^{-6}. In *para*-dimethoxybenzene a similar splitting of 6×10^{-6} is observed for the protonated carbons (Lippmaa *et al.* 1978). Line shifts in the solid state have been observed in polyphenylene oxide (Schaefer *et al.* 1977). For the epoxy the peak splitting most likely arises from the three-bond removed methylene group, while the *c* peak is split by the methyl groups.

At higher temperatures the splittings in peaks *c* and *d* disappear and the resonance lines sharpen in general. The coalescence of peaks *c* and *d* indicates that the ring carbons are rapidly sampling at least two magnetic environments. The simultaneous averaging of *both c* and *d* peaks points to a motion of the phenyl group with respect to the backbone. Based on the coalescence point, the activation enthalpy is estimated at about 54 kJ/mol. This mechanism, the averaging out of two disparate shifts, may represent an extreme example of the more complex averaging within the polymer. We speculate that the phenyl reorientation allows freedom for more subtle, perhaps collective motions that provide a partial averaging over many slightly different conformations. From this standpoint, spectra are most highly resolved at the highest temperature, up to the point at which modulation of the dipolar interaction leads to lifetime broadening.

The methyl resonance (*i*) is an exception. At low temperatures it broadens and finally disappears (figure 7). J. R. Lyerla (personal communication, 1979) has observed similar disappearance of the methyl resonance in polymethylmethacrylate; at sufficiently low temperature the line reappears. In the epoxy the vestigial peak in the methyl region at 151 K is associated with the piperidine curing agent, present at the 21 mol.% level relative to the monomer. As the methyl reorientation slows down from its room temperature rate, the proton decoupling becomes more inefficient, as discussed in § 3 *a*. From the available rotating frame relaxation times for the methyl peak (Garroway *et al.* 1979 *b*) and the extrapolated $T_{1\rho}^{C}$ values below 243 K, the line width due to molecular modulation of the carbon–proton dipolar coupling may be estimated. (In the DGEBA monomer and in the epoxy cured with methylenedianiline, Larsen & Strange (1973 *a*, *b*) observed a proton $T_{1\rho}$ minimum at 143–153 K; on comparison with their data, extrapolation of the methyl $T_{1\rho}^{C}$ down to about 153 K is a reasonable approximation.) The observed methyl line width increases more or less in parallel with $(\pi T_{1\rho}^{C})^{-1}$; line widths range from 55 to about 450 Hz at 359 and 177 K, respectively, while the $T_{1\rho}^{C}$ contributions are 7 and 280 Hz (VanderHart *et al.* 1981). The inhomogeneous contribution, defined for convenience as the difference between the total line width and $(\pi T_{1\rho}^{C})^{-1}$, increases less rapidly, from 47 Hz (3.1×10^{-6}) to 170 Hz (11.3×10^{-6}). This 8×10^{-6} increase in inhomogeneous broadening at low temperature may reflect the

PHILOSOPHICAL TRANSACTIONS OF THE ROYAL SOCIETY A MATHEMATICAL, PHYSICAL & ENGINEERING SCIENCES

PHILOSOPHICAL TRANSACTIONS OF THE ROYAL SOCIETY A MATHEMATICAL, PHYSICAL & ENGINEERING SCIENCES

Downloaded from rsta.royalsocietypublishing.org

presence of inequivalent methyl groups that are separated by 5×10^{-6} in the crystalline form of the monomer; at higher temperature this inequivalence may be partly averaged out by the phenyl reorientation.

Additionally, the phenyl and methyl motions will modulate the respective chemical shift anisotropies and, in principle, reduce the efficiency of the magic angle spinning. For the methyl resonance, with small anisotropy, this effect is not large (perhaps 0.5×10^{-6}). Some of the breadth of the protonated carbon peaks in the cured epoxy may well derive from this; the maximum estimate for these carbons is 12×10^{-6}, from §3*b*.

4. Conclusions

We have sketched consequences of the competition of spin–spin relaxation (and the similar problem of transmitter phase noise) with the true spin–lattice relaxation due to molecular motion. For high-quality synthesizers, phase noise relaxation is not a problem for $T_{1\rho}$ relaxation times of seconds or less. In glassy polymers at ambient temperature it appears that readily obtainable r.f. field amplitudes are sufficient to allow spin–lattice processes to predominate. For less mobile systems, e.g. the crystalline portions of polyethylene and of polyoxymethylene, r.f. field strengths of 60 kHz are too weak. Various strategies are available to determine whether spin–lattice relaxation dominates: weak r.f. field dependence of the observed $T_{1\rho}^{C*}$; comparison with the directly measured spin–spin rate for that system or with the rate for a theoretical or experimental model system. For static samples, suppression of dipolar order by r.f. pulses will alter the rotating frame relaxation when spin–spin relaxation is large. However, the separation of the spin–lattice and spin–spin rotating frame relaxation processes is the only aspect that has been considered here. Further progress is needed in the *quantitative* interpretation of the spin–lattice relaxation rates.

Of the mechanisms that lead to line broadening, many are linear in B_0 so that increases in static field will leave unchanged the *fractional* resolution (in millionths). Such effects are susceptibility, misalignment and jitter in the magic angle, and a distribution in isotropic chemical shifts. The dynamic effects are somewhat less straightforward to inventory since they involve the decoupling frequency ω_{1H} and spinning rate Ω_{rot}, which are not immutably fixed to B_0. If spinning frequencies are achieved that are directly proportional to increases in B_0, then the fractional line width due to modulation of the chemical shift anisotropy by slow molecular motion ($\Omega_{rot}^2 \tau_c^2 \gg 1$) will decrease with increasing field (cf. (14)). At the corresponding relaxation minimum ($\Omega_{rot}\tau_c = 1$), however, the resolution is field independent.

For off-resonant proton decoupling the increase in the proton resonance offset at high static fields leads to a deterioration of fractional resolution in proportion to increases in B_0. This presumes that the r.f. fields are unchanged. Practical difficulties in achieving high r.f. fields, owing to the greater power requirements at high frequency, will further exacerbate the broadening.

The broadening due to inadequate decoupling power, albeit applied on resonance, is explicitly independent of B_0 and so the fractional resolution improves at high magnetic field. Since only about 40 kHz decoupling fields are required to reduce broadening to the order of 1 Hz for, say, polyethylene, further improvement is insignificant.

Resolution improvement may well occur when the broadening arises from the modulation of the carbon–proton dipolar coupling by molecular motion (equation (11)), since $T_{1\rho}^{C}$ is largely

PHILOSOPHICAL TRANSACTIONS OF THE ROYAL SOCIETY A MATHEMATICAL, PHYSICAL & ENGINEERING SCIENCES

PHILOSOPHICAL TRANSACTIONS OF THE ROYAL SOCIETY A MATHEMATICAL, PHYSICAL & ENGINEERING SCIENCES

Downloaded from rsta.royalsocietypublishing.org

independent of B_0. So, provided comparable r.f. field strength can be achieved at high frequency, the fractional resolution will improve as B_0. Substantial improvements may be restricted to protonated carbons near a deep $T_{1\rho}^{C}$ minimum where this mechanism surely dominates the line width. Furthermore, modest changes in temperature may provide for large improvements, as in figure 7.

The effect of a quadrupolar nucleus that is dipolar coupled to the observed spin was not considered here. If the quadrupolar energy is less than the Zeeman energy, this broadening diminishes at higher static field, where the quadrupolar spin aligns more nearly to the B_0 axis and so allows the magic angle spinning to reduce the heteronuclear coupling (Kundla & Alla 1979; Zumbulyadis *et al.* 1981). Also outside the scope of this paper is any consideration of static field inhomogeneity due to magnet design, even though such inhomogeneity plays a minor role in some spectra and results presented here.

In summary, for amorphous materials we do not expect major gains, if any, in fractional resolution at a higher static field; degradation will occur if decoupling field strengths diminish substantially. Present decoupling fields (40–60 kHz) are adequate at 1.4 T. To the extent that magnet inhomogeneity dominates, spectra of crystalline materials may well improve owing to the better magnet homogeneity that can apparently be obtained at high field; optimum resolution may require the use of single crystals to minimize susceptibility broadening. For amorphous polymers and perhaps for crystalline systems with anisotropic susceptibility, present-day spectra may already exhibit the highest possible resolution: these materials are a challenge to invent other more selective methods to elucidate still finer detail from the n.m.r. solid state spectra.

This research has been sponsored, in part, by the Naval Air Systems Command. The specimen of ultra-orientated polyethylene was kindly provided by Professor R. S. Porter of the University of Massachusetts. Thanks go to our colleagues G. C. Chingas of N.R.L. and A. J. Vega of DuPont for sharing their views on susceptibility effects.

References (Garroway *et al.*)

Ailion, D. C. & Slichter, C. P. 1965 *Phys. Rev.* A **137**, 232–245.
Andrew, E. R. 1959 *Arch. Sci., Genève* **12**, 103–108.
Bartuska, V. J., Maciel, G. E., Schaefer, J. & Stejskal, E. O. 1977 *Fuel, Lond.* **56**, 354–358.
Bloch, F. 1958 *Phys. Rev.* **111**, 841–853.
Bloembergen, N. & Sorokin, P. P. 1958 *Phys. Rev.* **110**, 865–875.
Bloembergen, N., Purcell, E. M. & Pound, R. V. 1948 *Phys. Rev.* **73**, 679–712.
Bloembergen, N., Shapiro, S., Pershan, P. S. & Artman, J. O. 1959 *Phys. Rev.* **114**, 445–459.
Demco, D. E., Tegenfeldt, J. & Waugh, J. S. 1975 *Phys. Rev.* B **11**, 4133–4151.
Doskočilová, D., Tao, D. D. & Schneider, B. 1975 *Czech. J. Phys.* B **25**, 202–209.
Drain, L. E. 1962 *Proc. Phys. Soc.* **80**, 1380–1382.
Earl, W. L. & VanderHart, D. L. 1979 *Macromolecules* **12**, 762–767.
Garroway, A. N. 1979 *J. magn. Reson.* **34**, 283–293.
Garroway, A. N., Moniz, W. B. & Resing, H. A. 1976 *Prepr. Div. org. Coatings Plastics Chem.* **36**, 133–138.
Garroway, A. N., Moniz, W. B. & Resing, H. A. 1979*a* *Am. chem. Soc. Symp. Ser.* **103**, 67–87.
Garroway, A. N., Moniz, W. B. & Resing, H. A. 1979*b* *Faraday Symp. chem. Soc.* **13**, 63–74.
Garroway, A. N., Ritchey, W. M. & Moniz, W. B. 1981 (In preparation.)
Hartmann, S. R. & Hahn, E. L. 1962 *Phys. Rev.* **128**, 2042–2053.
Jeener, J. 1977*a* Presented at Sixth International Symposium on Magnetic Resonance, Banff, Canada.
Jeener, J. 1977*b* Presented at Waterloo n.m.r. Summer School, Waterloo, Canada.
Kundla, E. & Alla, M. A. 1979 In *Proc. XX Congress Ampere*, Tallinn, p. 92. Berlin: Springer-Verlag.
Landolt, H. H. & Börnstein, R. 1967 In *Zahlenwerte und Funktionen*, vol. 2, pt 10, 6th edn, pp. 158–159. Berlin: Springer-Verlag.
Larsen, D. H. & Strange, J. H. 1973*a* *J. Polym. Sci. Polym. Phys.* **11**, 65–74.

Downloaded from rsta.royalsocietypublishing.org

Larsen, D. H. & Strange, J. H. 1973*b* *J. Polym. Sci. Polym. Phys.* **11**, 449–456.
Lippmaa, E., Alla, M. & Tuherm, T. 1976 In *Proc. XIX Congress Ampere*, Heidelberg, pp. 113–118.
Lippmaa, E. T., Alla, M. A., Pehk, T. J. & Engelhardt, G. 1978 *J. Am. chem. Soc.* **100**, 1929–1931.
Lowe, I. J. 1959 *Phys. Rev. Lett.* **2**, 285–287.
McArthur, D. A., Hahn, E. L. & Walstedt, R. E. 1969 *Phys. Rev.* **188**, 609–638.
McCall, D. W. & Douglass, D. C. 1965 *Appl. Phys. Lett.* **7**, 12–14.
Maricq, M. M. & Waugh, J. S. 1979 *J. chem. Phys.* **70**, 3300–3316.
Mehring, M. 1976 *High resolution NMR spectroscopy in solids* (*NMR: basic principles and progress*, vol. 11). Berlin: Springer-Verlag.
Meyer, D. G. 1970 *IEEE Trans. Instrum. Measmt* **IM-19**, 215–227.
Pines, A. & Shattuck, T. W. 1974 *J. chem. Phys.* **61**, 1255–1256.
Pines, A., Gibby, M. G. & Waugh, J. S. 1972 *Chem. Phys. Lett.* **15**, 373–376.
Pines, A., Gibby, M. G. & Waugh, J. S. 1973*a* *J. chem. Phys.* **56**, 1776–1777.
Pines, A., Gibby, M. G. & Waugh, J. S. 1973*b* *J. chem. Phys.* **59**, 569–590.
Pourquie, J. F. J. M. & Wind, R. A. 1976 *Phys. Lett.* A **55**, 347–349.
Resing, H. A., Garroway, A. N. & Hazlett, R. N. 1978 *Fuel, Lond.* **57**, 450–454.
Rhim, W.-K., Pines, A. & Waugh, J. S. 1970 *Phys. Rev. Lett.* **25**, 218–220.
Sarles, L. R. & Cotts, R. M. 1958 *Phys. Rev.* **111**, 853–859.
Schaefer, J. & Stejskal, E. O. 1976 *J. Am. chem. Soc.* **98**, 1031–1032.
Schaefer, J., Stejskal, E. O. & Buchdahl, R. 1977 *Macromolecules* **10**, 384–405.
Schaefer, J., Stejskal, E. O., Steger, T. R., Sefcik, M. D. & McKay, R. A. 1980 *Macromolecules* **13**, 1121–1127.
Shoaf, J. H., Halford, D. & Risley, A. S. 1973 *Nat. Bur. Stand. tech. Note*, no. 632. Washington, D.C.: U.S. Department of Commerce.
Stejskal, E. O., Schaefer, J. & Steger, T. R. 1979 *Faraday Symp. chem. Soc.* **13**, 56–62.
Stokes, H. T. & Ailion, D. C. 1977 *Phys. Rev.* B **15**, 1271–1282.
Strombotne, R. L. & Hahn, E. L. 1964 *Phys. Rev.* A **133**, 1616–1629.
Suwelack, D., Rothwell, W. P. & Waugh, J. S. 1980 *J. chem. Phys.* **73**, 2559–2569.
Terao, T., Maeda, S. & Matsui, S. 1981 (In preparation.)
VanderHart, D. L. & Garroway, A. N. 1979 *J. chem. Phys.* **71**, 2773–2787.
VanderHart, D. L., Earl, W. & Garroway, A. N. 1981 *J. magn. Reson.* (Submitted.)
Veeman, W. S. 1979 *Faraday Symp. chem. Soc.* **13**, 179–180.
Veeman, W. S., Menger, E. M., Ritchey, W. & deBoer, E. 1979 *Macromolecules* **12**, 924–927.
Zumbulyadis, N., Young, R. S. & Henrichs, P. M. 1981 (In preparation.)

Discussion

W. S. Veeman (*University of Nijmegen, The Netherlands*). The authors and others have shown that in polymers the ^{13}C $T_{1\rho}$ is made up contributions of spin–lattice relaxation by molecular motions and of spin–spin relaxation due to proton dipolar fluctuations. Can the spin–spin contribution to $T_{1\rho}$ be eliminated by multiple-pulse n.m.r. on the protons during the carbon spin lock? If so, would this not be the clue to study polymeric motion at relative low frequencies?

A. N. Garroway. Suppression of proton spin fluctuations by multiple-pulse sequences (or variants of Lee–Goldburg off-resonance irradiation) should, in principle, reduce the spin–spin contributions to the observed carbon rotating frame relaxation. In such an experiment, one must take great care to minimize any cross-relaxation from the carbon to the effective multiple-pulse ('toggling') proton spin-lock system: such cross-polarization could occur even in the absence of spin fluctuations as in, for example, cross-polarization by the isotropic J coupling in liquids. One should probably use large proton r.f. fields and short multiple-pulse cycle times. To be sure, because of the exponential variation of the rotating frame spin–spin contribution on dipolar fluctuation time, spin–spin fluctuations need be slowed by only a factor of two or so to attenuate substantially spin–spin relaxation at moderate r.f. fields ($\omega_{1C}\tau_d \geqslant 1$).

Such a quenching of spin diffusion has already been demonstrated in the related experiments of separated local fields (Vaughan and Waugh) and self-decoupling (Mehring and Pines). Indeed Dr Veeman's own experience with polyoxymethylene shows that spin fluctuations can be slowed in that polymer by magic angle spinning rates of only 3–5 kHz.